PROCEEDINGS B

royalsocietypublishing.org/journal/rspb

Research

Cite this article: Chen B *et al*. 2022 Sensory evolution in a cavefish radiation: patterns of neuromast distribution and associated behaviour in *Sinocyclocheilus* (Cypriniformes: Cyprinidae). *Proc. R. Soc. B* **289**: 20221641. https://doi.org/10.1098/rspb.2022.1641

Received: 20 August 2022
Accepted: 22 September 2022

Subject Category:
Evolution

Subject Areas:
behaviour, ecology, evolution

Keywords:
troglomorphy, stygomorphy, cave biology, constructive traits, phylogeny

Author for correspondence:
Madhava Meegaskumbura
e-mail: madhava_m@mac.com

Electronic supplementary material is available online at https://doi.org/10.6084/m9.figshare.c.6233242.

THE ROYAL SOCIETY PUBLISHING

Sensory evolution in a cavefish radiation: patterns of neuromast distribution and associated behaviour in *Sinocyclocheilus* (Cypriniformes: Cyprinidae)

Bing Chen[1,2], Tingru Mao[1], Yewei Liu[1], Wenzhang Dai[3], Xianglin Li[1], Amrapali P. Rajput[1], Marcio R. Pie[4], Jian Yang[5], Joshua B. Gross[6] and Madhava Meegaskumbura[1]

[1]Guangxi Key Laboratory for Forest Ecology and Conservation, College of Forestry, Guangxi University, Nanning 530004, People's Republic of China
[2]Ministry of Education Key Laboratory for Biodiversity Science and Ecological Engineering, Institute of Biodiversity Science, Center of Evolutionary Biology, School of Life Sciences, Fudan University, Shanghai 200438, People's Republic of China
[3]School of Life Science and Institute of Wetland Ecology, Nanjing University, Nanjing 210000, People's Republic of China
[4]Biology Department, Edge Hill University, Ormskirk, Lancashire L39 4QP, UK
[5]Key Laboratory of Environment Change and Resource Use, Beibu Gulf, Nanning Normal University, Nanning, Guangxi, People's Republic of China
[6]Department of Biological Sciences, University of Cincinnati, Cincinnati OH 45221, USA

BC, 0000-0002-5259-7086; TM, 0000-0002-1942-1353; YL, 0000-0003-4712-1072; MRP, 0000-0002-2949-4871; JBG, 0000-0002-0032-1053; MM, 0000-0002-4599-6724

The genus *Sinocyclocheilus*, comprising a large radiation of freshwater cavefishes, are well known for their presence of regressive features (e.g. variable eye reduction). Fewer constructive features are known, such as the expansion of the lateral line system (LLS), which is involved in detecting water movements. The precise relationship between LLS expansion and cave adaptation is not well understood. Here, we examine morphology and LLS-mediated behaviour in *Sinocyclocheilus* species characterized by broad variation in eye size, habitat and geographical distribution. Using live-staining techniques and automated behavioural analyses, we examined 26 *Sinocyclocheilus* species and quantified neuromast organ number, density and asymmetry within a phylogenetic context. We then examined how these morphological features may relate to wall-following, an established cave-associated behaviour mediated by the lateral line. We show that most species demonstrated laterality (i.e. asymmetry) in neuromast organs on the head, often biased to the right. We also found that wall-following behaviour was distinctive, particularly among eyeless species. Patterns of variation in LLS appear to correlate with the degree of eye loss, as well as geographical distribution. This work reveals that constructive LLS evolution is convergent across distant cavefish taxa and may mediate asymmetric behavioural features that enable survival in stark subterranean microenvironments.

1. Background

Cavefishes are valuable model systems for understanding the evolution of adaptive features [1–4] because the cave environment presents extreme and constant pressures, such as limited food and perpetual darkness. These selective pressures are associated with common regressive changes such as vision and pigmentation loss [5,6]. However, constructive features have also evolved in cave-dwellers, often including the enhancement of non-visual senses [7]. The lateral line system (LLS) is one such non-visual sensory system composed of peripherally distributed neuromast organs. These organs are composed of

sensory hair cells harbouring a ciliary bundle (composed of a kinocilium and multiple stereocilia) surrounded by support cells [8,9]. In the head (cephalic) region, there are two types of neuromasts: larger canal neuromasts (CNs) that are contained within fluid-filled canals embedded with bones and superficial neuromasts that are found on the skin [10,11].

Other cave-dwelling species show significant modifications to the LLS. For instance, in the Mexican tetra (*Astyanax mexicanus*), cave-adapted morphs have more, and larger, neuromast organs compared to closely related surface-dwelling morphs. Additionally, cave morphs demonstrate a more asymmetric distribution of neuromasts on the head compared to surface morphs [12]. At present, the functional relevance of this asymmetry in sensory distribution in cave-dwelling animals is unclear. It may, however, facilitate a number of behavioural features of cave-adapted fishes, including lateral swimming preferences and wall-following behaviour [7,13–17].

Here, we sought to examine variation in the LLS among species in a species-rich genus, the *Sinocyclocheilus*. This genus provides a unique opportunity to examine morphological features, and putative behavioural correlates, in the context of many independently derived *Sinocyclocheilus* cavefishes comprised species showing variation in eye size, habitat type and geography [18,19].

Roughly one-third of the world's known cavefish species are endemic to China (148 species) [20], including those in the genus *Sinocyclocheilus* (Cypriniformes: Cyprinidae), which encompasses 75 known species [21]. These fishes are distributed across a vast karstic area of approximately 62 000 km^2 in the provinces of Yunnan, Guizhou and the Guangxi Zhuang Autonomous Region [22–24]. A prior study established that *Sinocyclocheilus* species can be divided into three categories based on eye morphology: normal-eyed, micro-eyed and eyeless. Mao *et al*. [19] showed that these three groups (quantified based on standardized eye diameter) often correlate to habitat use. Specifically, eyeless (also called 'blind') cavefishes are mostly obligate cave-dwellers (i.e. 'stygobitic'), meaning that they never leave the cave environment as adults. Micro-eyed cavefishes are mostly facultative cave-dwellers (i.e. 'stygophilic'), meaning they move among the cave, transitional and surface habitats. Finally, normal-eyed *Sinocyclocheilus* exclusively reside in surface waters [19]. Interestingly, however, eye morphology was not uniformly associated with these habitats (e.g. certain eyeless species are stygophilic), underscoring the complex evolutionary histories and ecological correlates of this genus. Nevertheless, this species-rich radiation enables a robust analysis, across multiple dimensions, to examine putative relationships between neuromast features and lateral line-mediated behaviours. While a prior study in *Sinocyclocheilus* investigated neuromasts comparing a single surface-dwelling species with an obligate cave-dwelling species [17], here we performed analysis of 26 species within the genus.

Since neuromasts may provide functional compensation for vision loss, we hypothesized that more extreme eye loss may be correlated with expansion of the LLS. Therefore, we examined three principal features: numerical variation and area covered by neuromasts, lateral distribution of neuromasts, left-right asymmetry and behavioural differences in wall-following. We predicted that eye size would be inversely correlated to numbers and area of neuromasts. Additionally, we predicted cave-dwellers (both obligate and facultative) would show higher distributional asymmetry of neuromasts compared to surface species, either due to selection (e.g. for lateral swimming preference) or neutral forces (e.g. relaxed selection on maintaining symmetry). Finally, we predicted that the more extreme cave-adapted fishes would show more lateralized swimming behaviours.

Interestingly, we found that the distribution of neuromasts was asymmetric across all groups, but the degree of asymmetry was more pronounced for species with 'regressed' eyes (i.e. inclusive of micro-eyed and eyeless). We also found that eyeless cave-adapted species show the most robust wall-following behaviour. Collectively, this work provides a comprehensive examination of LLS evolution in the highly diverse cave-adapted genus *Sinocyclocheilus*. In this context, our work further clarifies the complex relationships between environmental pressures of the cave and the evolution of constructive features.

2. Methods

(a) Fish collection and husbandry

Adult fishes were collected from the field between 2017 and 2020 across the Yunnan and Guizhou Provinces, and the Guangxi Zhuang Autonomous Region of China (figure 1; see geographical coordinates in electronic supplementary material: electronic supplementary material, table S1 and figure S1). All fishes were categorized based on eye morphology which was quantified using the sED metric (standardized eye diameter: the ratio of eye diameter to standard length, SL). Species were placed into three groups: (i) 'normal-eyed' = typical eye size and structure, sED > 3.0 mm; (ii) 'micro-eyed' = eyes and lens were measurable but significantly regressed, sED ≤ 3.0 mm and (iii) 'eyeless' = eyes were completely absent and unmeasurable (i.e. described as 'blind' in Mao *et al*. [19]). All fishes were maintained in an automated fish husbandry system (pH: 7.0–8.0, temperature 19 ± 1°C, dissolved oxygen 8.5 mg l^{-1}) without light. For this study, 76 representative individuals from 26 *Sinocyclocheilus* species (*approx*. 35% of species in the genus) were used (table 1). For comparison, we also examined individuals ($n = 3$ each) from two closely related species, *Carassius auratus* and *Cyprinus carpio* [25].

(b) Vital staining of neuromasts

To visualize neuromasts, live fish were immersed in 25 µg ml^{-1} DASPEI (D0815; Sigma-Aldrich) dissolved in 1 l of water [12,26,27]. Fish were first anaesthetized by exposure in a sterile solution of MS-222 (10–20 µg ml^{-1}; E808894-5g; Macklin) for 3–6 min, followed by brief immersion in ice water for approximately 20 s, depending on size of the individual (e.g. smaller specimens were exposed to ice water for shorter periods).

(c) Quantification of neuromast asymmetry and distribution patterns

Here we focused specifically on the head region, defined as the area rostral to the opercular and interopercular bones, exclusive of the lateral gill (figure 2*m*) [23]. Imaging was performed using a Leica M165FC stereomicroscope equipped with epifluoresence, using three fluorescent filters: Blue (470/40 nm excitation), Texas Red (560/40 nm excitation) and Green (546/10 nm excitation). Dorsal lateral, left-lateral and right-lateral aspects of each individual were imaged under identical conditions. High-definition 'montage' images were obtained following automated alignment by 'flattening' 30 images collected in the z-plane (× 9/13/16 magnification) using LASX (Leica) or Helicon Focus Pro v7.6.1 imaging software. The outlines of each fish and associated neuromast positions were obtained using the 'pencil' and 'point' tools in GIMP v2.10.24

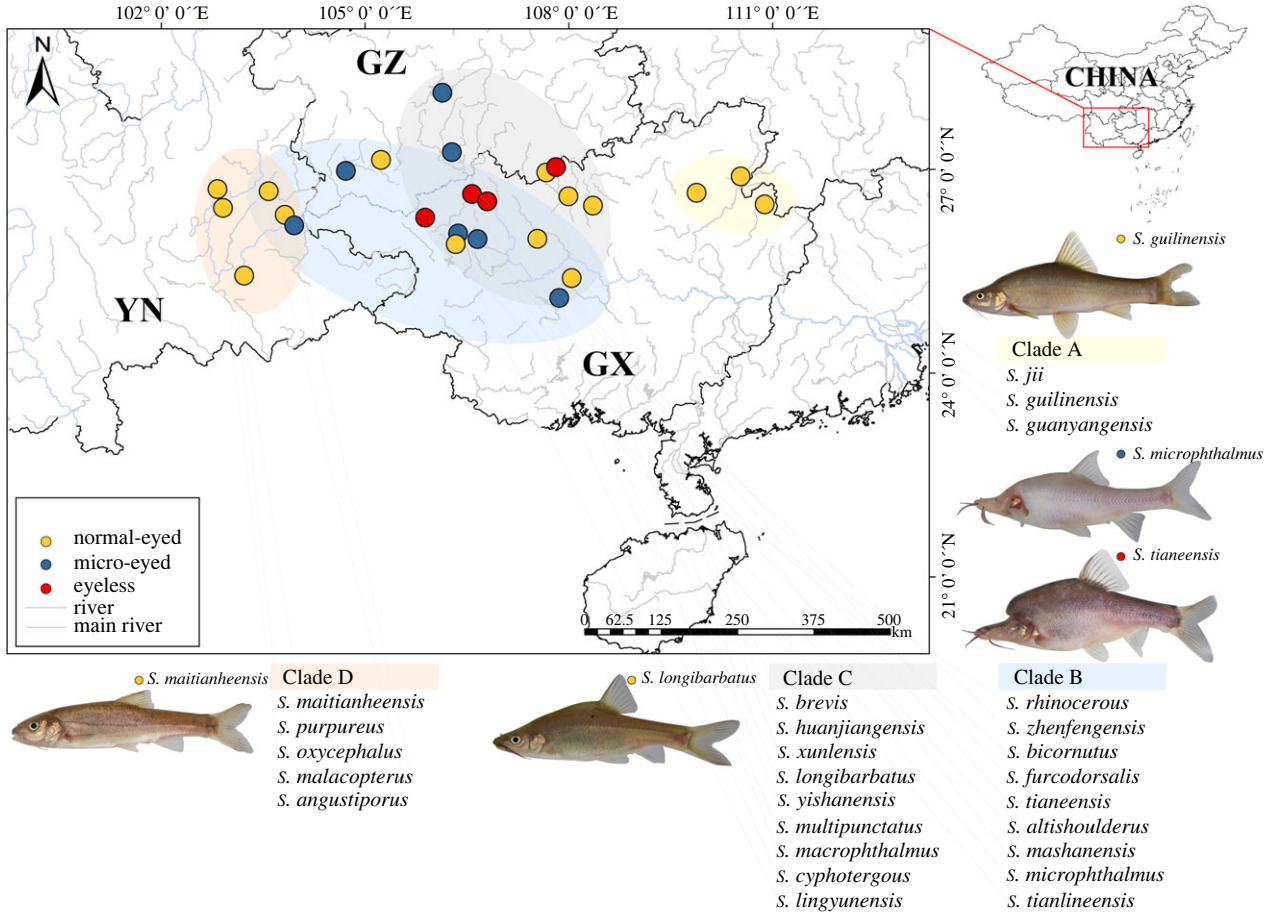

Figure 1. Map of sampling sites for 26 species of *Sinocyclocheilus*. Four main clades (*a–d*) are depicted alongside categorical eye morphology (normal-eyed, yellow dot; micro-eyed, blue dot; and eyeless, red dot) for each species. Representative images of individuals from each clade are shown. These include the early-emerging Clade A in the eastern range of Guangxi (yellow transparent oval), the western Clade D distribution in Yunnan (orange transparent oval) and Clades B (blue transparent oval) and C (grey transparent oval) in the intervening geographical range inclusive mainly of Guangxi and Guizhou. Provinces: GZ = Guizhou; YN = Yunnan; Guangxi Zhuang Autonomous Region = GX). (Online version in colour.)

(figure 2*g–i*). Neuromast numbers were quantified using ' Find Maxima', an automated cell counting feature and 'Measure' feature in FIJI (as described in [28]). All area measurements were illustrated from flattened montage images by outlining each region, using the 'measure' function and converting to mm^2. The SLs of all specimens were collected using a Vernier calliper.

To examine symmetry of neuromast positions across the left-right axis, we superimposed fluorescent images of neuromasts within each individual by performing a horizontal reflection of the left-lateral images. This involved identifying overlap of positions for neuromasts on the right and left sides of the head, as described in [29]. We then implemented the 'colocalization' [30] and 'JACop' [31] plugins in FIJI to calculate an overlap coefficient (OC) [12,32] based on the frequency of overlap between sides (left, right). This value represents the 'asymmetry value' (OC, figure 2*n*) of neuromasts for each individual ($OC \leq 0.4$ represents as asymmetry patterns [33]). Finally, to measure the relative clustering between neuromasts across species, we employed 'Delaunay Voronoi' triangulation (FIJI) to quantify the mean distance between neuromasts (annotated as 'DEL') that represents the 'density', as described in [34,35] (figure 2*j–l*).

(d) Phylogenetic comparative analyses

We divided the 26 species into three categories based on eye morphology (see above) yielding the following: normal-eyed ($n = 45$), micro-eyed ($n = 21$) and eyeless ($n = 12$). Importantly, a few species did not have uniform eye sizes across individuals (e.g. *S. guanyangensis*) [23]. In these cases, we selected individuals displaying the most common eye phenotype in this species (e.g. 'normal-eyed'). For these analyses, we used an established phylogenetic tree (see Mao *et al*. [19], electronic supplementary material, methods) on which we mapped quantifiable constructive features.

To understand the broader patterns of neuromast evolution across different species of *Sinocyclocheilus*, we also performed ancestral state reconstructions using maximum likelihood ('phytools' v1.0-1 [36]) in R. The first trait we examined was numerical bias of head neuromasts (i.e. which side of the head harboured more neuromast organs). This lateral bias trait was scored by calculating a signed asymmetry rate (SAR), $SAR = (R - L)/(R + L) * 100\%$; [37]. This analysis yielded two morphological categories: 'right-biased' ($SAR > 0$), in which more neuromasts are on the right-side and 'left-biased' ($SAR < 0$) in which more neuromasts are on the left side of the head (figure 3; electronic supplementary material, table S1 and figure S2). We next examined the distribution of neuromasts on the head, scored as the triangulation value from our 'Delaunay Voronoi' analyses. This metric of neuromast distribution provided a mean distance between neuromast per unit area of the head, yielding two groups: 'sparsely distributed' neuromasts (where $DEL > 0.2$) and 'densely distributed' (where $DEL \leq 0.2$) [27]. The third trait we examined was left-right asymmetry of neuromast distributions (i.e. OC, see above). Herein, 'absolute-asymmetry' was defined as instances where $OC < 0.1$, and 'slight-asymmetry' were instances where $OC \geq 0.1$. Next, we examined how neuromast trait differences between normal-eyed and regressed-eyed (micro-eyed + eyeless) groups by performing a set of Spearman's rank correlation analyses. The variables we examine included: (i) number of neuromasts, (ii) distributional area occupied

Table 1. Summary of the 26 *Sinocyclocheilus* species grouped according to eye morphology (normal-eyed, micro-eyed, eyeless), habitat (stygobitic, stygophilic, surface), clade (A, B, C and D) and geography (province). Clades A–D are as described in Mao *et al*. [19]. Provinces: Yunnan = YN, Guizhou = GZ, Guangxi Zhuang Autonomous Region = GX).

	stygobitic	stygophilic	surface
normal-eyed	*S. guilinensis* - A, GX	*S. longibarbatus* - C, GZ	
	S. jii - A, GX		
	S. guanyangensis - A, GX		*S. angustiporus* - D, YN
	S. zhenfengensis - B, GZ		*S. oxycephalus* - D, YN
	S. huanjiangensis - C, GX		*S. malacopterus* - D, YN
	S. macrophthalmus - C, GX		*S. purpureus* - D, YN
	S. brevis - C, GX		*S. maitianheensis* - D, YN
	S. lingyunensis - C, GX		
	S. yishanensis - C, GX		
micro-eyed	*S. mashanensis* - B, GX	*S. multipunctatus* - C, GZ	
	S. altishoulderus - B, GX		
	S. microphthalmus - B, GX		
	S. bicornutus - B, GZ		
	S. rhinocerous - B, YN		
	S. cyphotergous - C, GZ		
eyeless	*S. furcodorsalis* - B, GX		
	S. tianlinensis - B, GX		
	S. tianeensis - B, GX		
	S. xunlensis - C, GX		

by neuromasts, (iii) asymmetry value—OC, (iv) mean distance between neuromasts, (v) area of the head occupied by the eyes and (vi) SL. All neuromast scores were subjected to parametric one-way ANOVA with a *post hoc* Tukey test analysis. Non-parametric analyses were subjected to Wilcoxon signed-rank test (two-tailed, Holm correction) or a Kruskal–Wallis test with a *post hoc* Dunnett test analysis (two-tailed, Bonferroni correction). Unless otherwise stated, all statistical analyses were carried out in R v.3.6.3 [38], and significance for each test was set at $p < 0.05$. All graphs were created using package 'ggplot2' v3.3.5 [39].

(e) Behavioural analyses

To examine the potential role of neuromast traits on behaviour, we carried out a series of behavioural assays using 14 species ($n = 3$ individuals per species). These included 'normal-eyed' species (*S. guilinensis*, *S. longibarbatus*, *S. macrophthalmus*, *S. oxycephalus*, *S. zhenfengensis*, *S. purpureus* and *S. maitianheensis*); 'micro-eyed' (*S. mashanensis*, *S. microphthalmus*, *S. bicornutus* and *S. multipunctatus*) and 'eyeless' (*S. furcodorsalis*, *S. tianlinensis* and *S. tianeensis*). Each individual was acclimatized for 30 min in a rectangle arena (45 × 28 × 28 cm) in fresh, conditioned system water. An infrared camera (Canon XF405) captured video under infrared light in a sound-proof, dimly lit room (frame rate: 25.00P, 1280 × 720, 8 Mbps).

These studies focused on wall-following, an established behaviour associated with lateral line sensation in other cave-dwelling fishes. This behaviour was scored based on the length of time, and the facing side (left or right), of continuous swimming within a minimum distance from the tank wall. The distance employed was tank wall, less than 0.5 SL per individual from the wall, following the methods of Sharma *et al*. and Patton *et al*. [40,41]. For each assay, we recorded normal swimming for 10 min to observe wall-following and then added a barrier (an opaque cylinder, diameter 5 cm) for 5 min and recorded the side with which the individual approached the barrier [42–44]. All behavioural studies were analysed using EthoVision XT (v15.0, Noldus) alongside direct visual monitoring. This approach enabled us to both establish the presence of wall-following behaviour and determine the frequency of lateral approaches to the barrier.

3. Results and discussion

Animals living in perpetual darkness frequently lose vision while enhancing non-visual sensory systems. In other cave-adapted fishes, the lateral line sensory system is enhanced through increased numbers of peripheral sensory organs (neuromasts) [42,45,46]. In other species systems, this sensory expansion is lateralized [12,47–50], manifested as an asymmetric distribution and/or number of sensory organs. While the precise function of this asymmetry is unclear, it may be a consequence of relaxed pressure to maintain symmetry in an organism in the absence of vision. Alternatively, non-visual sensory asymmetry may be adaptive, by mediating lateral behavioural preferences that have been demonstrated in cavefishes. Here we found that many of the same features are present among species in the large *Sinocyclocheilus* lineage, suggesting that environmental pressures within the cave microenvironment influence the evolution of both sensory expansion and asymmetry.

(a) Patterns of neuromast asymmetry

In other cave-dwelling species, neuromast asymmetry demonstrates a consistent left-side bias (e.g. *A. mexicanus* cave-adapted morphs from North America) or a right-side bias (*Gasterosteus aculeatus* from Central America) [37,51].

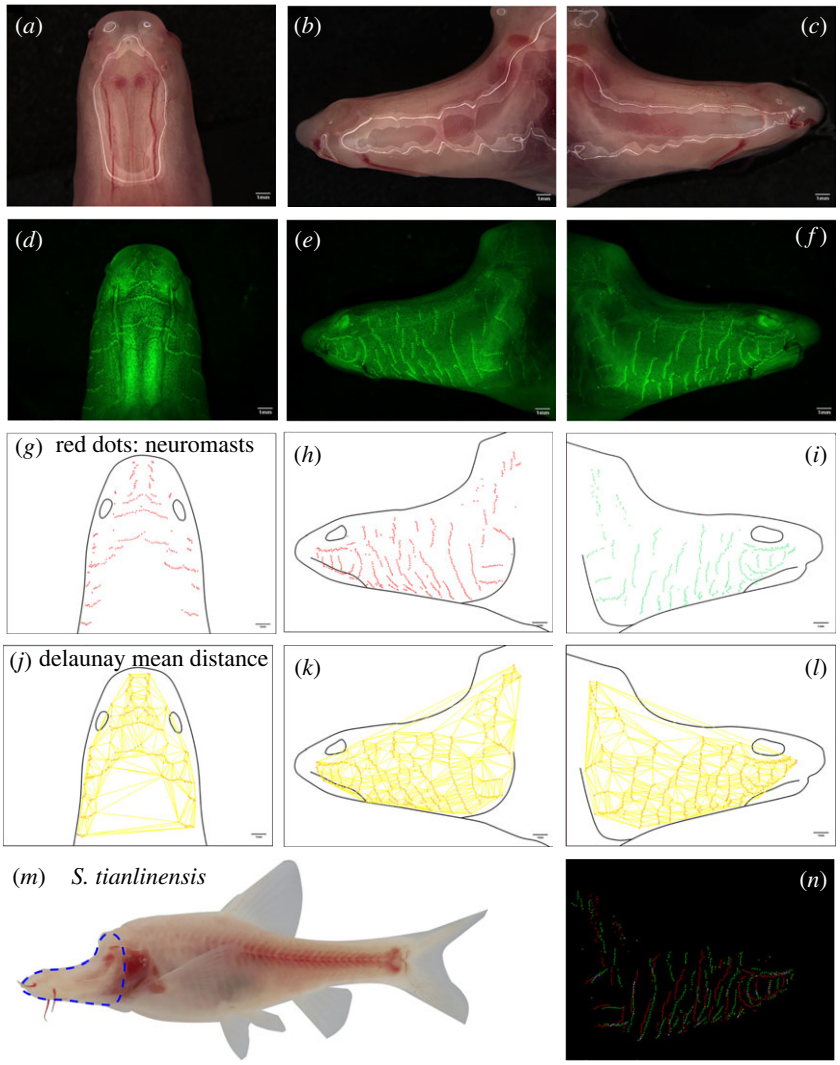

Figure 2. Imaging, quantification and data collection from a representative *Sinocyclocheilus* individual. A representative *S. tianlinensis* is bright-field and fluorescent imaged in the dorsal (*a*,*d*), left-lateral (*b*,*e*) and right-lateral (*c*,*f*) aspects. The areas of each aspect of the head were collected (black lines, (*g–i*)) and the precise positions of each superficial neuromast were recorded (red dots, (*g–i*)) based on DASPEI-positive signals from each fluorescent image (green, (*d–f*)). The mean distance between all head neuromasts was calculated using Delaunay Voronoi triangulation (yellow lines, (*j–l*); see Methods). The area of the head scored in each individual (blue dotted lines, (*m*)) was compared for left- and right-sided positions of neuromasts (red and green dots, (*n*)). The overlap in position of neuromasts, i.e. the 'OC' for each individual was quantified (e.g. OC = 0.086) using the JACop feature in FIJI. Scale = 1.0 mm. (Online version in colour.)

Neuromast distributions in our analysis revealed asymmetry was present across the left-right axis, and this variation was present within and across species. OCs indicated that all *Sinocyclocheilus* species showed some degree of asymmetry (figure 4; electronic supplementary material, table S2), while neither of the cyprinid outgroups showed comparable levels of asymmetry. Notably, with respect to eye morphology, the three groups we examined (normal-eyed, micro-eyed and eyeless) failed to show statistically significant differences in asymmetry scores. This may suggest that sensory asymmetry is a putatively ancestral feature of this genus. Having said this, we do note that normal-eyed species were marginally more symmetric, particularly compared to eyeless species (mean ± s.d.: normal-eyed = 0.098 ± 0.050; micro-eyed = 0.096 ± 0.027; H_2 = 0.64, $p > 0.05$; eyeless = 0.091 ± 0.031; electronic supplementary material, table S6).

In comparing asymmetry among clades within *Sinocyclocheilus*, we discovered that Clade D (uniformly comprised normal-eyed, surface-dwelling species) showed the least asymmetry (mean ± s.d. = 0.119 ± 0.058). Alternatively, Clade C (comprised species with both reduced- and normal-eyes) demonstrated the most asymmetry (mean ± s.d. = 0.079 ± 0.031). This finding consistent with prior work suggesting asymmetry facilitates navigation in darkness [52,53], food-foraging success [54] and the ability to maximize sensory information [37,51]. We note, however, that there was modest within-species variation for some Clades (see bar lengths in Clade A, figure 4), but substantial within-species variation for others (see bar lengths in Clade D, figure 4). We also note that Clade D (composed exclusively of normal-eyed fishes) were among the most asymmetric species, implying that neuromast asymmetry is likely not a simple function of visual system loss. Rather, the evolutionary history of this clade may have supported an adaptive relevance to lateral line asymmetry that is unrelated to the environmental pressures within a cave.

(b) Numerical variation and lateral distribution of neuromasts

Unexpectedly, there were significantly fewer neuromasts in eyeless species compared to normal- and micro-eyed species (mean ± s.d.: normal-eyed = 1859 ± 504; micro-eyed = 2252 ± 802; eyeless = 1543 ± 248; $H_2 = 10$, $p = 0.007$, electronic

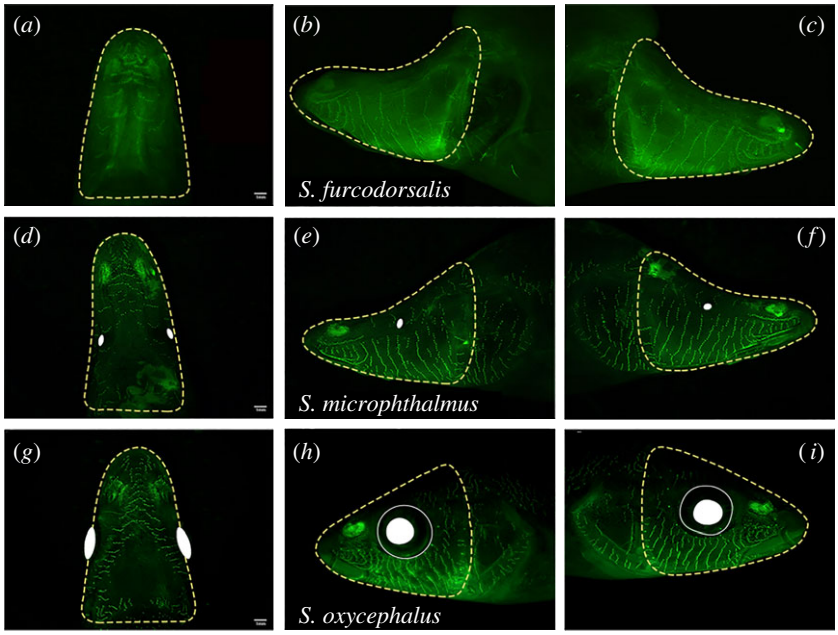

Figure 3. Fluorescent neuromast labelling in *Sinocyclocheilus* groups demonstrating three distinct eye morphologies. A representative eyeless species, *S. furcodorsalis* (Clade B from Guangxi), shown in the dorsal (*a*), left-lateral (*b*) and right-lateral (*c*) aspects. This species demonstrates absolute asymmetry of head neuromasts (biased to the right side), which are sparsely distributed. A representative micro-eyed species, *S. microphthalmus* (Clade B from Guangxi), shown in the dorsal (*d*), left-lateral (*e*) and right-lateral (*f*) aspects. *S. microphthalmus* demonstrates slight asymmetry (biased to the left side) of head neuromasts, which are sparsely distributed. A representative normal-eyed species, *S. oxycephalus* (Clade D from Yunnan), shown in the dorsal (*g*), left-lateral (*h*) and right-lateral (*i*) aspects. This species demonstrates slight asymmetry (biased to the right side) of head neuromasts, which are densely distributed. Yellow dotted line around head represent the area under consideration, solid white cycles show the eye ball and the white cycles show the eye orbit. Scale = 1 mm. (Online version in colour.)

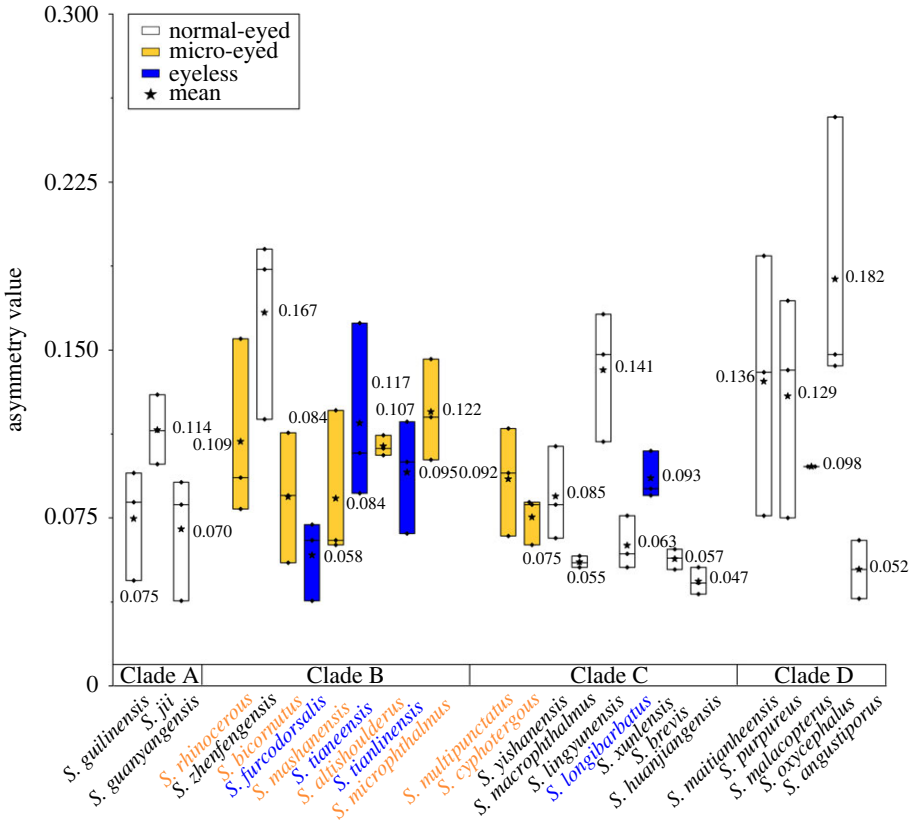

Figure 4. Four clades of *Sinocyclocheilus* demonstrate group-level variation in lateral line sensory asymmetry. Substantial variation exists in lateral asymmetry based on calculated asymmetry values across 26 species of *Sinocyclocheilus* with eye morphology variation. We found a trend towards higher symmetry from Clades A–D, composed which are composed of normal-eyed (white), micro-eyed (yellow) and eyeless (blue) species. Note variation within each species was modest for some Clades (see bar lengths in Clade A), but substantial for others (see bar lengths in Clade D). We note, however, that Clade A (similarly composed exclusively of normal-eyed fishes) were among the most asymmetric species, suggesting that neuromast asymmetry is likely not a simple function of visual system loss. A lower value represents higher asymmetry. For statistical results, see electronic supplementary material, tables S2 and S6. (Online version in colour.)

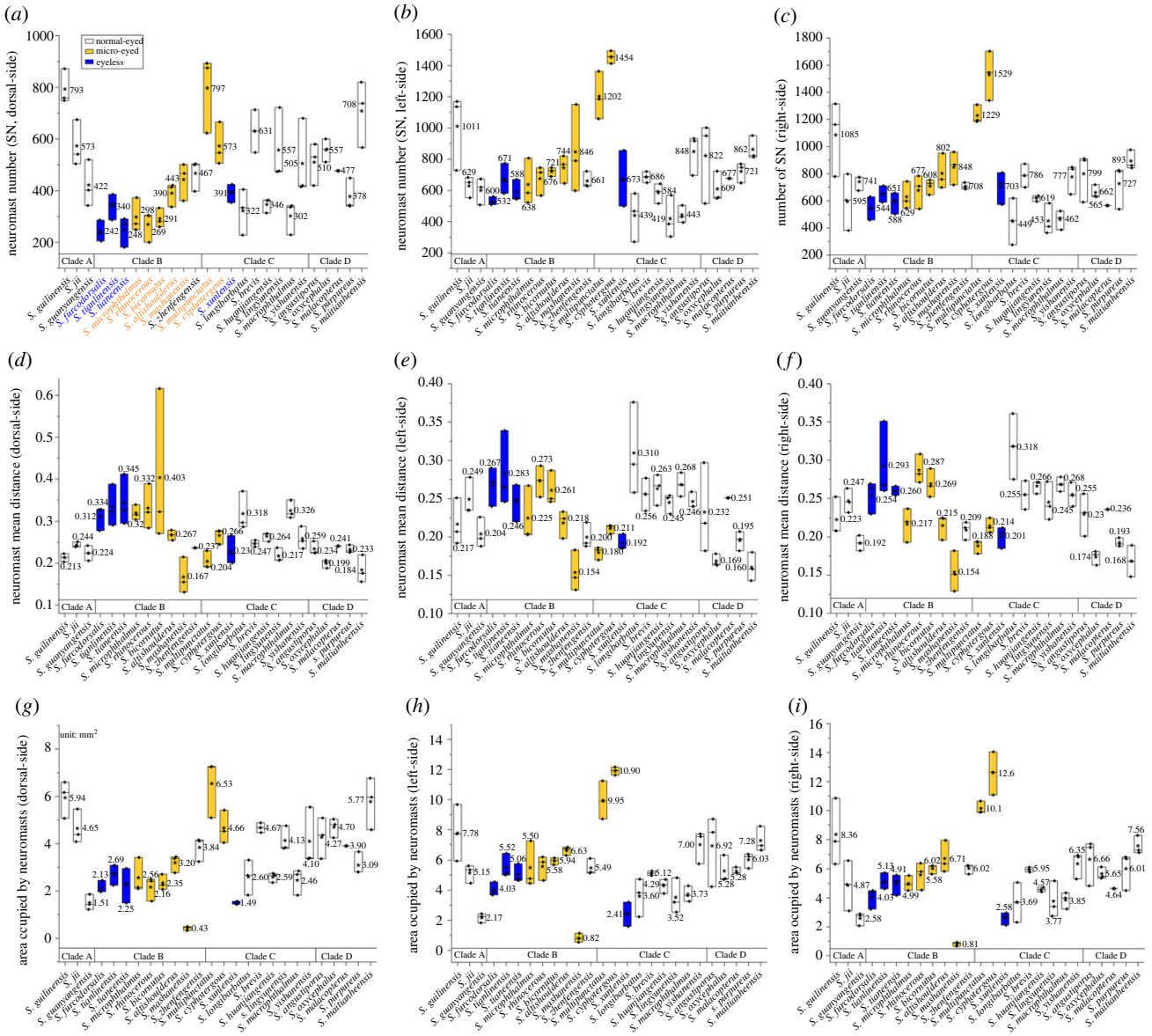

Figure 5. The area, number and mean distance between neuromasts across four clades of *Sinocyclocheilus* reveal deep trends in sensory lateralization. Our comprehensive analyses examined the number of neuromasts on the head in the dorsal (*a*), left-lateral (*b*) and right-lateral aspects (*c*). Additionally, we compared the mean distance between neuromasts in the dorsal (*d*), left-lateral (*e*) and right-lateral aspects (*f*). Finally, we compared the head areas populated by neuromasts on the dorsal (*g*), left-lateral (*h*) and right-lateral aspects (*i*). Normal-eyed fishes are represented in white, micro-eyed fishes in yellow and eyeless fishes in blue histograms (mean value = asterisks, ends of histograms = s.d.). (Online version in colour.)

supplementary material, table S6), in contrast with other systems. Namely, surface morphs of the *Astyanax* mexicanus have fewer and more sparsely distributed neuromasts compared to cave morphs [12,55].

In the dorsal aspect of the head, all species had fewer neuromasts compared to the lateral sides of the head (figure 5*a–c*). Eyeless fishes had the fewest dorsal neuromasts, normal-eyed fishes had the most and micro-eyed fishes were intermediate (mean ± s.d.: normal-eyed = 503 ± 155; micro-eyed = 437 ± 194; eyeless = 305 ± 77; $H_2 = 16.5$, $p < 0.001$, figure 6*a*; electronic supplementary material, table S6). A potential explanation for this may be that obligate subterranean fishes experience relaxed predation pressures, e.g. from birds [22,56], compared to surface-dwelling fishes. However, a few dorsal neuromasts may be necessary for navigation within caves [57]. A notable exception from this pattern was *S. lingyunensis* for which more neuromasts were found on the dorsal surface of head (mean dorsal = 557, left = 419, right = 453). In the lateral aspect, normal-eyed and eyeless fishes had higher counts on the right-side, while micro-eyed species had more neuromasts on the left-side (figure 6*b*).

With respect to the relative density of neuromasts (figure 5*d–f*), we found that dorsal neuromasts are the most sparsely distributed across groups, especially in eyeless species (mean ± s.d. of DEL: normal-eyed = 0.24 ± 0.04; micro-eyed = 0.28 ± 0.10; eyeless = 0.31 ± 0.06; $H_2 = 12$, $p = 0.002$; figure 6*c*; electronic supplementary material, table S6). On the lateral surfaces of the head, neuromasts also tended to be sparser on the right compared to the left sides for all groups (figure 6*d*).

We then examined the area occupied by neuromasts and compared this feature across groups (figure 5*g–i*). In the dorsal head, we a significantly smaller area was populated by neuromasts in eyeless species compared to normal- and micro-eyed species (mean ± s.d.; normal-eyed = 3.88 ± 1.33; micro-eyed = 3.13 ± 1.94; eyeless = 2.14 ± 0.59; $H_2 = 15.9$, $p < 0.001$; figure 6*e*). The distributional area of neuromasts across the left and right sides were also comparable across species, but normal-eyed species had the largest area, micro-

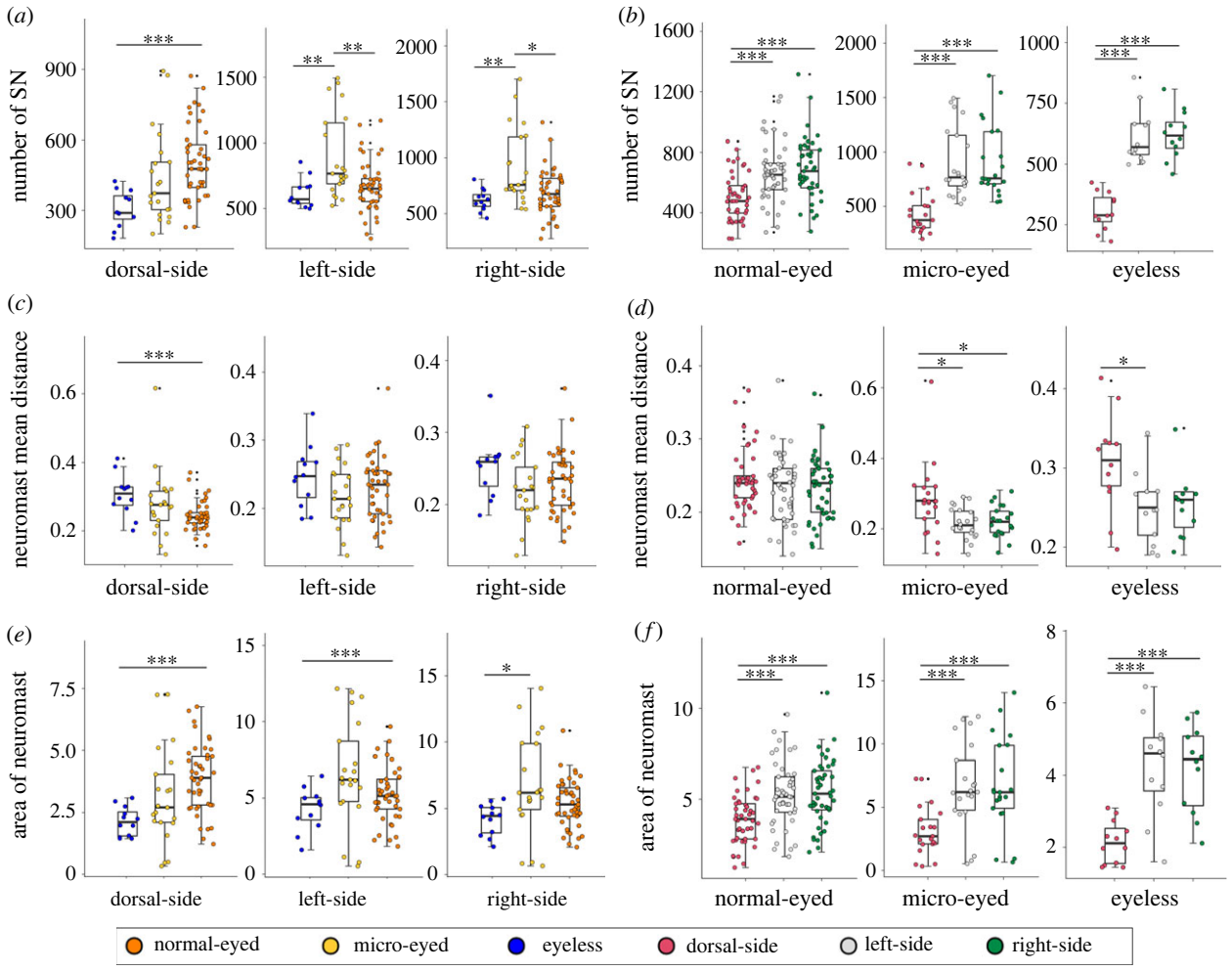

Figure 6. Statistical comparisons comparing the dorsal, left- and right-lateral heads for several features reveal significant trends based on eye morphology. We examined the non-parametric statistical relationship between neuromast features comparing normal-eyed (orange), micro-eyed (yellow) and eyeless (blue) *Sinocyclocheilus* across the dorsal, left-lateral and right-lateral heads (*a*,*c*,*e*). Additionally, we compared non-parametric statistical test values within each morphology group focusing on the dorsal (red), left (grey) and right (green) aspects (*b*,*d*,*f*). The neuromast features included the number of superficial neuromasts (*a*,*b*), the mean distance between neuromasts (*c*,*d*) and the area of the head populated by neuromasts (*e*,*f*). *: $p < 0.05$, **: $p < 0.01$ and ***: $p < 0.001$. All statistical results are provided in the electronic supplementary material, tables S2 and S6. (Online version in colour.)

eyed species were intermediate and eyeless species had the smallest areas (mean ± s.d.: normal-eyed = 14.49 ± 4.59; micro-eyed = 16.44 ± 8.80; eyeless = 10.56 ± 2.95; $F = 3.83$, $p = 0.026$; electronic supplementary material, table S6; figure 6*f*). Thus, although neuromast patterns of distribution are generally regarded as being more complex in eyeless species [17], this does not appear to be the case uniformly across *Sinocyclocheilus*.

Eyeless *Sinocyclocheilus* species have fewer CNs compared to normal-eyed species (median: normal-eyed = 17, micro-eyed = 13; eyeless = 5; electronic supplementary material, table S6). Surprisingly, no CNs were observed in *S. rhinocerous* and *S. cyphotergous* (electronic supplementary material, table S2), suggesting that the canal LLS may have regressed in these species. In distantly related species, surface populations tend to show highly stereotypical numbers and positions of CNs, while cave [49] and derived [58,59] populations are quite variable.

In sum, neuromasts are mostly reduced in number and in area of distribution in eyeless species of *Sinocyclocheilus*. Unexpectedly, micro-eyed species had the most neuromasts, a larger distributional area, and more densely clustered neuromasts than species in the other two groups. These relatively augmented features may have evolved as a consequence of micro-eyed forms being subjected to heterogeneous selective pressures since they encounter surface, subterranean and transitional habitats [23,60,61]. Conversely, eyeless *Sinocyclocheilus* species appear to have adapted to the subterranean habitat using fewer neuromasts. It should be noted, however, that although eyeless species, e.g. *S. tianlinensis*, have fewer neuromasts, each organ has more sensory hair cells which may have improved the neurobiological sensitivity to detect higher frequency detection [17,62,63]. Thus, although this species harbours fewer sensory organs, sensory expansion may have evolved through an alternative route of increased the receptive potential at the level of each sensory organ.

(c) Correlations between asymmetry and eye morphology

We found that the area within which neuromasts were distributed was positively correlated with the number of neuromasts ($\rho = 0.77$, $p < 0.001$). Unsurprisingly, the mean distance between neuromasts (i.e. the density of neuromasts, more distance = less dense) was inversely correlated to the number of neuromasts ($\rho = -0.63$, $p < 0.001$). Interestingly, it appears that patterns of sensory asymmetry are most evident based on the relative clustering of neuromasts (electronic supplementary material, table S7). Species with regressed eyes were more asymmetric than normal-eyed species, albeit

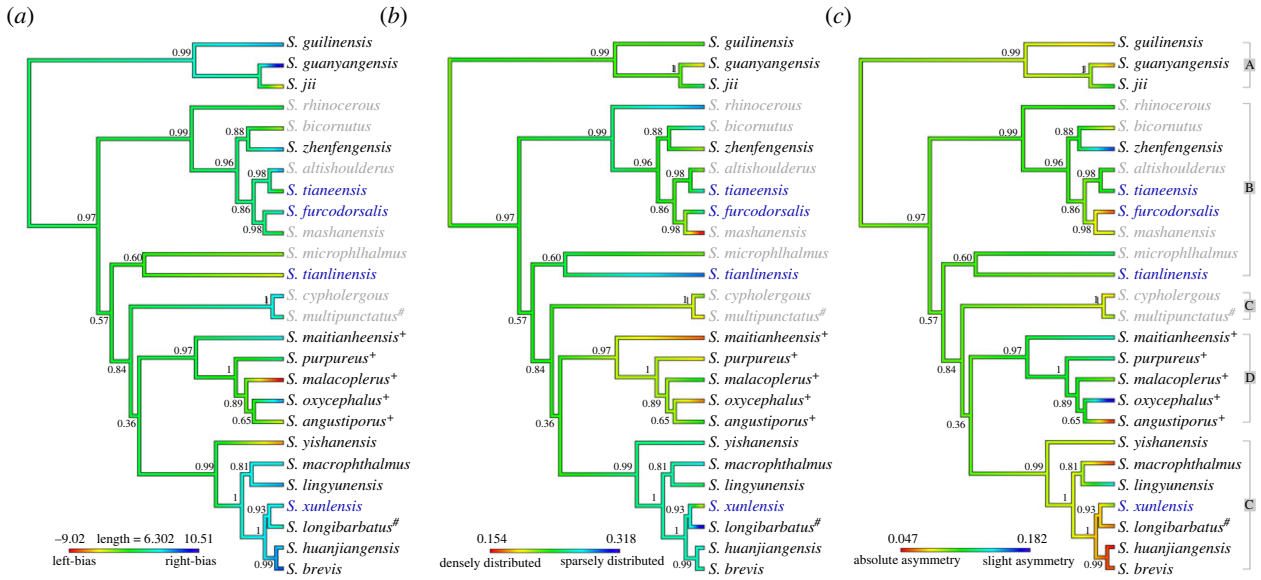

Figure 7. Patterns of neuromast features are informed through depictions in a phylogenetic context. Ancestral state reconstruction using maximum likelihood for symmetry (*a*) lateral bias (left versus right side), (*b*) neuromast distribution (sparse versus dense) and (*c*) neuromast symmetry (absolute versus slight). A colour gradient map shows the reconstructed phenotypic trait values in the context of *Sinocyclocheilus* phylogenetic relationships. Branch colours correspond to the degree of asymmetry, lateral bias and distribution. Four major clades (A, B, C and D) are shown on the right. Normal-eyed species are depicted in black, micro-eyed species in blue and eyeless species in grey. Stygophilic habitat denoted with 'hash' (#), surface habitat with 'plus' (+), and unlabelled branches are stygobitic. (Online version in colour.)

with more sparsely distributed neuromasts. This finding may indicate that loss of vision in *Sinocyclocheilus* is broadly associated with sparser, and more asymmetrically distributed, neuromast organs. The lower density of neuromast distribution may be an optimization to provide the lower resolution of information for living in stable environment (distinguishing a wall or a ceiling, as opposed to a predator). At present, however, it remains unclear precisely what is the functional relevance of this pattern in the cave microenvironment [37].

(d) Patterns of neuromast evolution

We performed an ancestral reconstruction of the three principal neuromast traits examined in this study: numerical variation, neuromast distributions (i.e. sparse or dense) and symmetry of lateral distributions (figure 7). Examining these traits in the context of a phylogenetic analysis reveals that these traits do not necessarily evolve in concert (electronic supplementary material, tables S3–S5), but show complex patterns across lineages. For example, while asymmetry was associated with the evolution an eyeless species such as *S. furcodorsalis*, it was not associated with that of a different eyeless species (*S. tianlinensis*; figure 7*a*). Similar incongruities were found for the polarity of asymmetric differences, i.e. whether a bias was towards the left or right (figure 7*b*), as well as neuromast distributions. We feel these results imply that complex trends in neuromast, of lateral line evolution has occurred independently across these lineages, likely in response to diverse selective pressures acting on each species and perhaps together with developmental plasticity.

(e) Wall-following behaviour in *Sinocyclocheilus*

Our behavioural assays revealed that eyeless species navigate markedly differently from normal- and micro-eyed species. Both normal-eyed and eyeless *Sinocyclocheilus* species prefer to use the lateral side with more neuromasts for wall-following behaviour (wall-following time, mean ± s.d.: normal-eyed = 87.87 ± 66.59 in left, 76.97 ± 50.75 in right; eyeless = 150.55 ± 81.29 in left, 122.91 ± 66.39 in right, see electronic supplementary material, table S6; figure 8*f*). Specifically, normal-eyed and eyeless species have more neuromasts on the left side of their heads and perform wall-following behaviour from the left-side more frequently (mean ± s.d.: normal-eyed = 11 ± 8 in left, 10 ± 7 in right; eyeless = 19 ± 10 in left, 16 ± 10 in right; figure 8*g*; electronic supplementary material, table S6). By contrast, micro-eyed *Sinocyclocheilus* species showed no differences between left and right sides.

In summary, eyeless species demonstrated a more restricted pattern of tank usage for wall-following behaviour, but with more increased activity. Conversely, sighted species used the entire arena space with more random swimming patterns (figure 8*c–e*′). Wall-following behaviour has also been characterized in *A. mexicanus*; however, eyeless morphs orient their lateral side with fewer neuromasts towards the wall, while perhaps using the opposite side for detecting stimuli important for feeding, communication and spatial learning [14,42]. Eyeless *Sinocyclocheilus* species show a similar pattern of asymmetry; however, herein the side with more neuromasts appears to be essential for mediating this lateral preference [64].

4. Conclusion

Sinocyclocheilus is an old species complex, with an estimated age of approximately 10–11 My [19,65]. These species are distributed across a vast karstic expanse spanning three provinces in southern China [22]. Prior work shows that one of the major drivers of speciation in this group was isolation over long periods of time, suggesting geographical speciation has dominated this radiation [19,66,67]. These divergences occurred during the geological uplift of the Yunnan–Kweichow Plateau alongside with the aridification

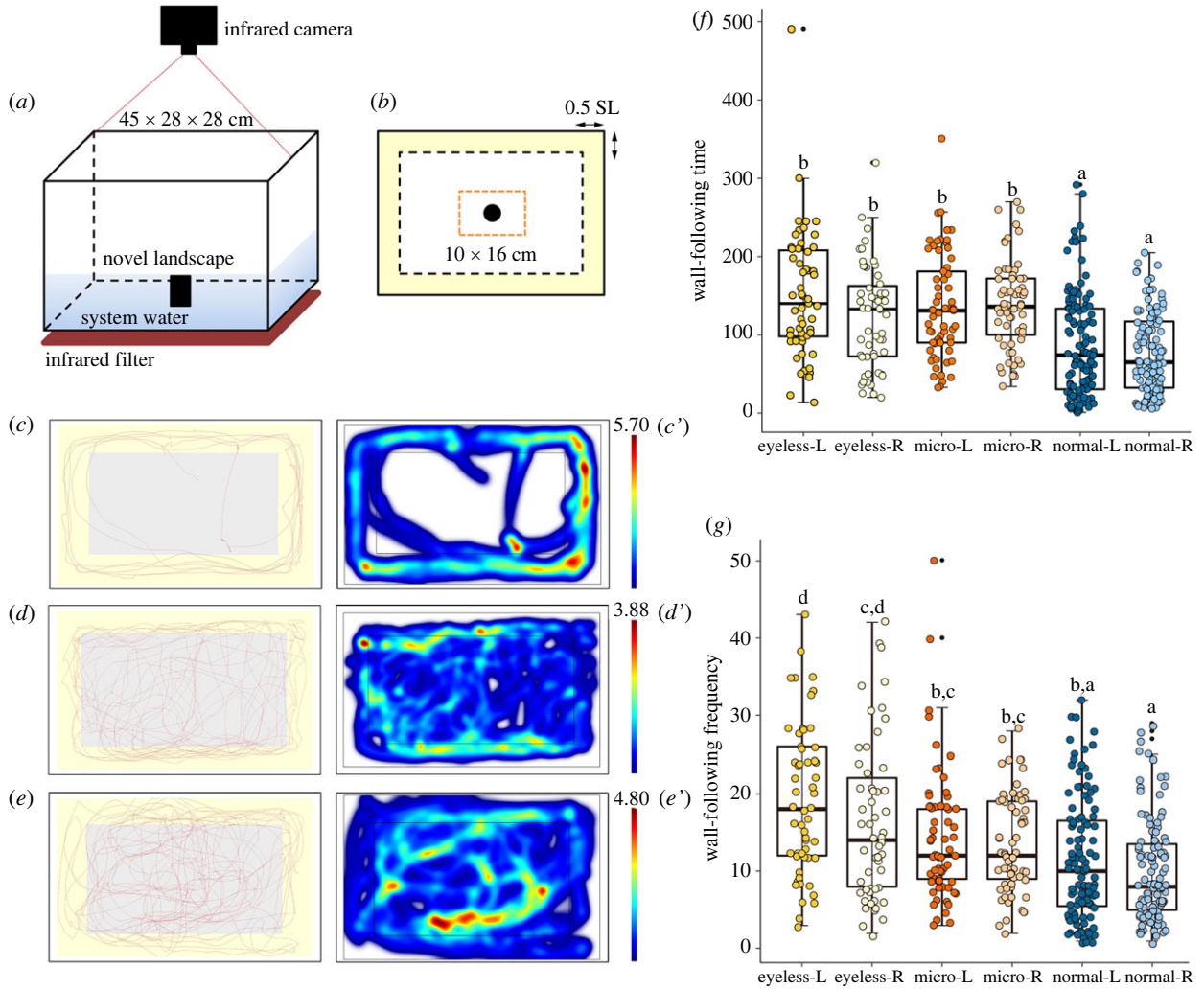

Figure 8. Different species of Sinocyclocheilus demonstrate distinct wall-following behaviour associated with eye morphology. Our assay system recorded infrared video of swimming behaviour in a novel landscape with an aeration pump indicated by a black rectangle (*a*). The assayed tank region included an area (pale yellow) depicting the near-wall region. The orange-dotted region indicates the area of the tank in which a novel obstruction was placed. Representative swimming traces (red lines) are shown for 10 min of wall-following behaviour assay for an eyeless species (*c*,*c*′; *S. tianeensis*), a micro-eyed species (*d*,*d*′; *S. microphthalmus*) and a normal-eyed fish (*e*,*e*′; *S. macrophthalmus*). Plots were generated from EthoVision XT. Heatmaps generated from each trial represent the total time (min) a fish remained in one place where warmer colours denote a longer time, and cooler colours denote a shorter time (*c*′–*e*′). Histograms depict the relative differences in the amount of time spent for wall-following (*f*) and frequency of wall-following (g) tracking both left and right side for all trials. (Online version in colour.)

of China, which occurred during the Pliocene and Pleistocene eras [66]. We feel the diverse variation we discovered in neuromast evolution in these fishes likely evolved through a complex set of influences reflecting this isolation and vast geographical distribution.

In addition to some trends in lateral line evolution, we found substantial variation in many neuromast features. This variation may well be adaptive, given the complexity of navigating life in markedly different habitats. For example, neuromast asymmetry was mostly biased to the right-side with expansion; for almost all species, neuromasts on the dorsal surface of head were less numerous than the lateral sides of the head. Species with regressed eyes (micro-eyed and eyeless) showed more asymmetry than the normal-eyed forms. However, we found the most neuromast variation in micro-eyed species that encounter both cave and surface environments. Wall-following assays further underscore the likely association with behavioural evolution between cave-adapted species, given the clear differences between normal-eyed and eyeless species. Although the relevance of these behavioural differences is incompletely understood, lateral sensation may facilitate adaptive habitat exploration in total darkness. Finally, several patterns of neuromast distribution and swimming behaviour are convergent with other distantly related cavefishes species, underscoring the importance of non-visual sensory expansion to survive the starkness of the cave microhabitat.

Ethics. The project was approved by Guangxi Autonomous Region Government and Guangxi University Ethical Clearance Committee (protocol number: GXU-2021-125 and 2022-GXU-005).

Data accessibility. Raw data for this study are available from the Dryad Digital Repository (https://doi.org/10.5061/dryad.w0vt4b8t3) [68].

The data are provided in the electronic supplementary material [69].

Authors' contributions. B.C.: conceptualization, data curation, formal analysis, investigation, methodology, validation, visualization, writing—original draft and writing—review and editing; T.M.: formal analysis, investigation, visualization, writing—original draft and writing—review and editing; Y.L.: data curation, investigation, methodology, validation and writing—review and editing; W.D.: data curation, investigation, visualization and writing—review and editing; X.L.: data curation, formal analysis, investigation and writing—review and editing; A.P.R.: data curation, formal analysis, investigation, validation, writing—original draft and writing—review and editing; M.R.P.: formal analysis, investigation, methodology, writing—original draft and writing—review and editing; J.Y.:

funding acquisition, investigation, resources, supervision and writing—review and editing; J.B.G.: conceptualization, investigation, methodology, supervision, writing—original draft and writing—review and editing; M.M.: conceptualization, funding acquisition, investigation, resources, supervision, writing—original draft and writing—review and editing.

All authors gave final approval for publication and agreed to be held accountable for the work performed therein.

Conflict of interest declaration. We declare no conflicts of interest.

Funding. This work was supported by the Startup funding for M.M. though Guangxi University for fieldwork, laboratory work and student support. National Natural Science Foundation of China (grant no. 31860600) to J.Y. for laboratory and fieldwork. B.C., T.M. and Y.L. were supported also by Innovation Project of Guangxi Graduate Education YCBZ2021008. These funding bodies played no role in the design of the study and collection, analysis and interpretation of data or in the writing of the manuscript.

Acknowledgements. We thank the following individuals and institutions: Noldus (Netherlands) for providing access to EthoVision XT software; members of EED lab for their cooperation and support and Christopher J. Schneider (Boston University) comments on manuscript.

References

1. Jeffery WR. 2001 Cavefish as a model system in evolutionary developmental biology. *Dev. Biol.* **231**, 1–12. (doi:10.1006/dbio.2000.0121)
2. Berti R, Durand JP, Becchi S, Brizzi R, Keller N, Ruffat G. 2001 Eye degeneration in the blind cave-dwelling fish *Phreatichthys andruzzii*. *Can. J. Zool.* **79**, 1278–1285. (doi:10.1139/z01-084)
3. Jeffery WR. 2009 Regressive evolution in *Astyanax* cavefish. *Annu. Rev. Genet.* **43**, 25–47. (doi:10.1146/annurev-genet-102108-134216)
4. Niemiller ML, Fitzpatrick BM, Miller BT. 2008 Recent divergence with gene flow in Tennessee cave salamanders (Plethodontidae: *Gyrinophilus*) inferred from gene genealogies. *Mol. Ecol.* **17**, 2258–2275. (doi:10.1111/j.1365-294X.2008.03750.x)
5. Jeffery WR, Strickler AG, Guiney S, Heyser DG, Tomarev SI. 2000 *Prox 1* in eye degeneration and sensory organ compensation during development and evolution of the cavefish *Astyanax*. *Dev. Genes Evol.* **210**, 223–230. (doi:10.1007/s004270050308)
6. Wilkens H, Strecker U. 2003 Convergent evolution of the cavefish *Astyanax* (Characidae, Teleostei): genetic evidence from reduced eye-size and pigmentation. *Biol. J. Linn. Soc.* **80**, 545–554. (doi:10.1111/j.1095-8312.2003.00230.x)
7. Yoshizawa M, Jeffery WR. 2011 Evolutionary tuning of an adaptive behavior requires enhancement of the neuromast sensory system. *Commun. Integr. Biol.* **4**, 89–91. (doi:10.4161/cib.14118)
8. Cahn PH. 1989 The mechanosensory lateral line: neurobiology and evolution. *BioScience* **40**, 215–216. (doi:10.2307/1311373)
9. Webb JF, Shirey JE. 2003 Postembryonic development of the cranial lateral line canals and neuromasts in zebrafish. *Dev. Dynam.* **228**, 370–385. (doi:10.1002/dvdy.10385)
10. Smith S. 1996 Pattern formation in the urodele mechanoreceptive lateral line: what features can be exploited for the study of development and evolution? *Int. J. Dev. Biol.* **40**, 727–733. (doi:10.1016/0141-8130(96)01109-9)
11. Bird NC, Webb JF. 2014 Heterochrony, modularity, and the functional evolution of the mechanosensory lateral line canal system of fishes. *EvoDevo* **5**, 21. (doi:10.1186/2041-9139-5-21)
12. Gross JB, Gangidine A, Powers AK. 2016 Asymmetric facial bone fragmentation mirrors asymmetric distribution of cranial neuromasts in blind Mexican cavefish. *Symmetry* **8**, 118. (doi:10.3390/sym8110118)
13. Elipot Y, Hinaux H, Callebert J, Rétaux S. 2013 Evolutionary shift from fighting to foraging in blind cavefish through changes in the serotonin network. *Curr. Biol.* **23**, 1–10. (doi:10.1016/j.cub.2012.10.044)
14. Yoshizawa M. 2015 Behaviors of cavefish offer insight into developmental evolution. *Mol. Reprod. Dev.* **82**, 268–280. (doi:10.1002/mrd.22471)
15. Jiang Y, Peichel CL, Torrance L, Rizvi Z, Thompson S, Palivela VV, Pham H, Ling F, Bolnick DI. 2017 Sensory trait variation contributes to biased dispersal of threespine stickleback in flowing water. *J. Evol. Biol.* **30**, 681–695. (doi:10.1111/jeb.13035)
16. Simon V, Hyacinthe C, Rétaux S. 2019 Breeding behavior in the blind Mexican cavefish and its river-dwelling conspecific. *PLoS ONE* **14**, e0212591. (doi:10.1371/journal.pone.0212591)
17. Ma ZQ, Herzog H, Jiang YG, Zhao YH, Zhang DY. 2020 Exquisite structure of the lateral line system in eyeless cavefish *Sinocyclocheilus tianlinensis* contrast to eyed *Sinocyclocheilus macrophthalmus* (Cypriniformes: Cyprinidae). *Integr. Zool.* **15**, 314–328. (doi:10.1111/1749-4877.12430)
18. Yang JX *et al.* 2016 The *Sinocyclocheilus* cavefish genome provides insights into cave adaptation. *BMC Biol.* **14**, 1. (doi:10.1186/s12915-015-0223-4)
19. Mao TR, Liu YW, Meegaskumbura M, Yang J, Ellepola G, Senevirathne G, Fu C, Gross BJ, Pie MR. 2021 Evolution in *Sinocyclocheilus* cavefish is marked by rate shifts, reversals, and origin of novel traits. *BMC Ecol. Evol.* **21**, 45. (doi:10.1186/s12862-021-01776-y)
20. Zhao YH, Huang ZS, Huang JQ, Zhang CG, Meng FW. 2021 Phylogenetic analysis and expression differences of eye-related genes in cavefish genus *Sinocyclocheilus*. *Integr. Zool.* **16**, 354–367. (doi:10.1111/1749-4877.12466)
21. Jiang WS, Li J, Lei XZ, Wen ZR, Han YZ, Yang JX, Chang JB. 2019 *Sinocyclocheilus sanxiaensis*, a new blind fish from the Three Gorges of Yangtze River provides insights into speciation of Chinese cavefish. *Integr. Zool.* **16**, 354–367. (doi:10.24272/j.issn.2095-8137.2019.065)
22. Romero A, Zhao YH, Chen XY. 2009 The hypogean fishes of China. *Environ. Biol. Fish.* **86**, 211–278. (doi:10.1007/s10641-009-9441-3)
23. Zhao YH, Zhang CG. 2009 *Endemic fishes of Sinocyclocheilus (Cypriniformes: Cyprinidae) in China: species diversity, cave adaptation, systematics and zoogeography*. Beijing, China: Science Press.
24. Huang QH, Cai YL, Xing XS. 2008 Rocky desertification, antidesertification, and sustainable development in the karst mountain region of southwest China. *J. Hum. Environ.* **37**, 390–392. (doi:10.1579/08-S-493.1)
25. Tan M, Armbruster JW. 2018 Phylogenetic classification of extant genera of fishes of the order Cypriniformes (Teleostei: Ostariophysi). *Zootaxa* **4476**, 6–39. (doi:10.11646/zootaxa.4476.1.4)
26. Webb JF, Northcutt RG. 1997 Morphology and distribution of pit organs and canal neuromasts in non-teleost bony fishes. *Brain Behav. Evol.* **50**, 139–151. (doi:10.1159/000113328)
27. Powers AK, Berning DJ, Gross JB. 2020 Parallel evolution of regressive and constructive craniofacial traits across distinct populations of *Astyanax mexicanus* cavefish. *J. Exp. Zool. B Mol. Dev. Evol.* **334**, 450–462. (doi:10.1002/jez.b.22932)
28. Schindelin J *et al.* 2012 Fiji: an open-source platform for biological-image analysis. *Nat. Methods* **9**, 676–682. (doi:10.1038/nmeth.2019)
29. Palmer AR, Strobeck C, Chippindale AK. 1993 Bilateral variation and the evolutionary origin of macroscopic asymmetries. *Genetica* **89**, 201–218. (doi:10.1007/BF02424514)
30. Gorlewicz A, Krawczyk K, Szczepankiewicz AA, Trzaskoma P, Mulle C, Wilczynski GM. 2020 Colocalization colormap: an ImageJ Plugin for the quantification and visualization of colocalized signals. *Neuroinformatics* **18**, 661–664. (doi:10.1007/s12021-020-09465-9)
31. Cordelières F, Bolte S. 2008 JACoP v2.0: improving the user experience with co-localization studies. See https://imagej.net/imagej-wiki-static/JaCoP.
32. Dunn KW, Kamocka MM, McDonald JH. 2011 A practical guide to evaluating colocalization in biological microscopy. *Am. J. Physiol. Cell Physiol.* **300**, C723–C742. (doi:10.1152/ajpcell.00462.2010)
33. Zinchuk V, Grossenbacher Zinchuk O. 2009 Recent advances in quantitative colocalization analysis:

focus on neuroscience. *Prog. Histochem. Cytochem.* **44**, 125–172. (doi:10.1016/j.proghi.2009.03.001)

34. George PL, Borouchaki H. 1998 *Delaunay triangulation and meshing: application to finite elements*. Paris, France: Hermès.
35. Aurenhammer F, Klein R, Lee DT. 2012 *Voronoi diagrams and delaunay triangulations*. Singapore: World Scientific Press.
36. Revell LJ. 2012 Phytools: an R package for phylogenetic comparative biology (and other things). *Methods Ecol. Evol.* **3**, 217–223. (doi:10.1111/j.2041-210X.2011.00169.x)
37. Planidin NP, Reimchen TE. 2021 Ecological predictors of lateral line asymmetry in stickleback (*Gasterosteus aculeatus*). *Evol. Ecol.* **35**, 609–629. (doi:10.1007/s10682-021-10117-w)
38. Pinheiro J *et al* 2017 Package 'nlme': linear and nonlinear mixed effects models, version 3(1). See https://svn.r-project.org/R-packages/trunk/nlme/.
39. Wickham H. 2016 *Ggplot2: elegant graphics for data analysis*. New York, NY: Springer.
40. Sharma S, Coombs S, Patton P, de Perera TB. 2009 The function of wall-following behaviors in the Mexican blind cavefish and a sighted relative, the Mexican tetra (*Astyanax*). *J. Comp. Physiol. A* **195**, 225–240. (doi:10.1007/s00359-008-0400-9)
41. Patton P, Windsor S, Coombs S. 2010 Active wall-following by Mexican blind cavefish (*Astyanax mexicanus*). *J. Comp. Physiol. A* **196**, 853–867. (doi:10.1007/s00359-010-0567-8)
42. de Perera T B, Braithwaite VA. 2005 Laterality in a non-visual sensory modality—the lateral line of fish. *Curr. Biol.* **15**, 241–242. (doi:10.1016/j.cub.2005.03.035)
43. Jiang YG, Fu JC, Zhang DY, Zhao YH. 2016 Investigation on the lateral line systems of two cavefish: *Sinocyclocheilus Macrophthalmus* and *S. Microphthalmus* (Cypriniformes: Cyprinidae). *J. Bionic Eng.* **13**, 108–114. (doi:10.1016/S1672-6529(14)60164-5)
44. McGaugh SE *et al.* 2020 Evidence for rapid phenotypic and behavioural shifts in a recently established cavefish population. *Biol. J. Linn. Soc.* **129**, 143–161. (doi:10.1093/biolinnean/blz162)
45. Soares D, Niemiller ML. 2020 Extreme adaptation in caves. *Anat. Rec.* **303**, 15–23. (doi:10.1002/ar.24044)
46. Krishnan J, Rohner N. 2017 Cavefish and the basis for eye loss. *Phil. Trans. R Soc. Lond. B* **372**, 20150487. (doi:10.1098/rstb.2015.0487)
47. Dezfuli BS, Magosso S, Simoni E, Hills K, Berti R. 2009 Ultrastructure and distribution of superficial neuromasts of blind cavefish, *Phreatichthys andruzzii*, juveniles. *Microsc. Res. Tech.* **72**, 665–671. (doi:10.1002/jemt.20714)
48. Powers AK, Kaplan SA, Boggs TE, Gross JB. 2018 Facial bone fragmentation in blind cavefish arises through two unusual ossification processes. *Sci. Rep.* **8**, 7015. (doi:10.1038/s41598-018-25107-2)
49. Soares D, Niemiller ML. 2020 Variation in cephalic neuromasts surface and cave-dwelling fishes of the family Amblyopsidae (Teleostei: Percopsiformes). *J. Cave Karst Stud.* **82**, 198–209. (doi:10.4311/2019LSC0115)
50. Trokovic N, Herczeg G, Ghani NIA, Shikano T, Merilä J. 2012 High levels of fluctuating asymmetry in isolated stickleback populations. *BMC Evol. Biol.* **12**, 115. (doi:10.1186/1471-2148-12-115)
51. Fernandes VFL, Macaspac C, Lu L, Yoshizawa M. 2018 Evolution of the developmental plasticity and a coupling between left mechanosensory neuromasts and an adaptive foraging behavior. *Dev. Biol.* **441**, 262–271. (doi:10.1016/j.ydbio.2018.05.012)
52. Coombs S, Janssen J, Webb JF. 1988 Diversity of lateral line systems: evolutionary and functional considerations. In *Sensory biology of aquatic animals* (eds J Atema, RR Fay, AN Popper, WN Tavolga), pp. 553–593. New York, NY: Springer.
53. Montgomery JC, Coombs S, Baker CF. 2001 The mechanosensory lateral line system of the hypogean form of *Astyanax Fasciatus*. *Environ. Biol. Fish.* **62**, 87–96. (doi:10.1023/A:1011873111454)
54. Yamamoto Y, Byerly MS, Jackman WR, Jeffery WR. 2009 Pleiotropic functions of embryonic *sonic hedgehog* expression link jaw and taste bud amplification with eye loss during cavefish evolution. *Dev. Biol.* **330**, 200–211. (doi:10.1016/j.ydbio.2009.03.003)
55. Teyke T. 1990 Morphological differences in neuromasts of the blind cave fish *Astyanax hubbsi* and the sighted river fish *Astyanax mexicanus*. *Brain Behav. Evol.* **35**, 23–30. (doi:10.1159/000115853)
56. Zhao YH, Zhang CG. 2006 Past research and future development on endemic Chinese cavefish of the genus *Sinocyclocheilus* (Cypriniformes, Cyprinidae). *Acta Zootaxonomica Sin.* **31**, 769–777. (doi:10.3969/j.issn.1000-0739.2006.04.013)
57. He Y, Chen XY, Xiao TQ, Yang JX. 2013 Three-dimensional morphology of the *Sinocyclocheilus hyalinus* (Cypriniformes: Cyprinidae) horn based on synchrotron X-ray microtomography. *Zool. Res.* **34**, 128–134. (doi:10.11813/j.issn.0254-5853.2013.E4-5.E128)
58. Wark AR, Peichel CL. 2010 Lateral line diversity among ecologically divergent threespine stickleback populations. *J. Exp. Biol.* **213**, 108–117. (doi:10.1242/jeb.031625)
59. Planidin NP, Reimchen TE. 2022 Behavioural responses of threespine stickleback with lateral line asymmetries to experimental mechanosensory stimuli. *J. Exp. Biol.* **225**, jeb243661. (doi:10.1242/jeb.243661)
60. Zhao YH, Watanabe K, Zhang CG. 2006 *Sinocyclocheilus donglanensis*, a new cavefish (Teleostei: Cypriniformes) from Guangxi, China. *Ichthyol. Res.* **53**, 121–128. (doi:10.1007/s10228-005-0317-z)
61. Culver D, Pipan T. 2019 *The biology of caves and other subterranean habitats*. Oxford, UK: Oxford University Press.
62. Dinklo T, Van Netten SM, Marcotti W, Kros CJ. 2003 Signal processing by transducer channels in mammalian outer hair cells. In *Biophysics of the cochlea* (ed. A Gummer), pp. 73–80. Singapore: World Scientific Press.
63. McHenry MJ, van Netten SM. 2007 The flexural stiffness of superficial neuromasts in the zebrafish (*Danio rerio*) lateral line. *J. Exp. Biol.* **210**, 4244–4253. (doi:10.1242/jeb.009290)
64. Lunsford ET, Paz A, Keene AC, Liao JC. 2022 Evolutionary convergence of a neural mechanism in the cavefish lateral line system. *eLife* **11**, e77387. (doi:10.7554/eLife.77387)
65. Li ZQ, Guo BC, Li JB, He SP, Chen YY. 2008 Bayesian mixed models and divergence time estimation of Chinese cavefishes (Cyprinidae: *Sinocyclocheilus*). *Chin. Sci. Bull.* **53**, 2342–2352. (doi:10.1007/s11434-008-0297-2)
66. Xiao H, Chen SY, Liu ZM, Zhang RD, Li WX, Zan RG, Zhang YP. 2005 Molecular phylogeny of *Sinocyclocheilus* (Cypriniformes: Cyprinidae) inferred from mitochondrial DNA sequences. *Mol. Phylogenet. Evol.* **36**, 67–77. (doi:10.1016/j.ympev.2004.12.007)
67. Mao TR, Liu YW, Mariana MV, Pie MR, Gajaba E, Fu C, Yang J, Madhava M. 2022 Evolving in the darkness: phylogenomics of *Sinocyclocheilus* cavefishes highlights recent diversification and cryptic diversity. *Mol. Phylogenet. Evol.* **168**, 107400. (doi:10.1016/j.ympev.2022.107400)
68. Chen B *et al.* 2022 Sensory evolution in a cavefish radiation: patterns of neuromast distribution and associated behaviour in *Sinocyclocheilus* (Cypriniformes: Cyprinidae). *Dryad Digital Repository*. (doi:10.5061/dryad.w0vt4b8t3)
69. Chen B *et al.* 2022 Data from: Sensory evolution in a cavefish radiation: patterns of neuromast distribution and associated behaviour in *Sinocyclocheilus* (Cypriniformes: Cyprinidae). Figshare. (doi:10.6084/m9.figshare.c.6233242)